nature medicine

CAPON-nNOS coupling can serve as a target for developing new anxiolytics

Li-Juan Zhu[1,2,8], Ting-You Li[3,8], Chun-Xia Luo[1,2], Nan Jiang[3], Lei Chang[1,3], Yu-Hui Lin[1,2], Hai-Hui Zhou[1,2], Chen Chen[1,2], Yu Zhang[2], Wei Lu[4,7], Li-Yan Gao[1,2], Yu Ma[3], Qi-Gang Zhou[2], Qin Hu[5], Xiao-Ling Hu[6], Jing Zhang[2], Hai-Yin Wu[1,2] & Dong-Ya Zhu[1,2]

Anxiety disorders are highly prevalent psychiatric diseases[1,2]. There is need for a deeper understanding of anxiety control mechanisms in the mammalian brain and for development of new anxiolytic agents. Here we report that the coupling between neuronal nitric oxide synthase (nNOS) and its carboxy-terminal PDZ ligand (CAPON) can serve as a target for developing new anxiolytic agents. Augmenting nNOS-CAPON interaction in the hippocampus of mice by overexpressing full-length CAPON gave rise to anxiogenic-like behaviors, whereas dissociating CAPON from nNOS by overexpressing CAPON-125C or CAPON-20C (the C-terminal 125 or 20 amino acids of CAPON) or delivering Tat-CAPON-12C (a peptide comprising Tat and the 12 C-terminal amino acids of CAPON) in the hippocampus of mice produced anxiolytic-like effects. Mice subjected to chronic mild stress (CMS) displayed a substantial increase in nNOS-CAPON coupling in the hippocampus and a consequent anxiogenic-like phenotype. Disrupting nNOS-CAPON coupling reversed the CMS-induced anxiogenic-like behaviors. Moreover, small-molecule blockers of nNOS-CAPON binding rapidly produced anxiolytic-like effects. Dexamethasone-induced ras protein 1 (Dexras1)–extracellular signal–regulated kinase (ERK) signaling was involved in the behavioral effects of nNOS-CAPON association. Thus, nNOS-CAPON association contributes to the modulation of anxiety-related behaviors via regulating Dexras1-ERK signaling and can serve as a target for developing potential anxiolytics.

Anxiety disorders represent the most common of psychiatric diseases[1,2]. Selective serotonin reuptake inhibitors (SSRIs) and benzodiazepines (BZDs) are the most commonly prescribed anxiolytics. However, the severe side effects of BZDs and the fact that SSRIs take effect very slowly render their use problematic[3]. By exploring key mechanisms underlying anxiety control in mammalian brain, researchers may be able to develop new anxiolytics that are rapidly efficacious and clinically well tolerated.

nNOS mediates stress-related depressive behaviors, negatively regulates 5-HT1A receptor–mediated anxiolytic-like effects, controls aggressive behaviors and contributes to the genetic risk for schizophrenia[4–7]. It contains a PDZ domain[8] that can interact with a variety of other proteins, including post-synaptic density protein 95 (PSD-95)[9] and carboxy-terminal PDZ ligand of nNOS (CAPON)[10], a scaffolding protein that regulates dendrites[11] and synapses[12]. Variants of the gene encoding CAPON are associated with increased severity of post-traumatic stress disorder and depression[13].

The N-terminal phosphotyrosine-binding domain of CAPON binds to Dexras1. Dexras1 is activated by S-nitrosylation induced by nNOS in response to *N*-methyl-D-aspartate receptor (NMDAR) stimulation in brain. The nNOS-CAPON association facilitates nNOS activation of Dexras1 (ref. 8). In the brain, Dexras1 negatively regulates the phosphorylation of ERK[14], a kinase implicated in synaptogenesis[15,16] and emotional behaviors[17,18]. Overexpression of Dexras1 decreased phosphorylated ERK (pERK) in the hippocampus, and knockdown of Dexras1 increased pERK and produced anxiolytic-like effects (**Supplementary Fig. 1**). The NO donor DETA/NONOate caused anxiogenic-like behaviors (**Supplementary Fig. 2a–e**), whereas we previously observed that an nNOS inhibitor had anxiolytic-like effects[7]. Moreover, nNOS-CAPON association decreased pERK abundance and increased S-nitrosylation of Dexras1 (**Supplementary Fig. 2f,g**). We thus wondered whether nNOS-CAPON interaction modulates anxiety-related behaviors via NO-Dexras1-ERK signaling.

To test this hypothesis (**Fig. 1a**), we generated a lentiviral vector, LV-CAPON-L-GFP, that expresses full-length CAPON (CAPON-L), which is an adaptor protein between nNOS and its targets[10,19,20]. After microinjection into the hippocampus of ICR mice, LV-CAPON-L-GFP effectively infected the hippocampus, produced considerable CAPON-L-GFP (**Fig. 1b**) and significantly increased the amount of nNOS-CAPON complex *in vitro* and *in vivo* (**Fig. 1c**). It also caused the mice to display significantly increased latency to feed in a novel environment in the novelty-suppressed feeding (NSF) test and spend less time in the open arms in the elevated-plus-maze (EPM) test and in the lit compartment of a light-dark box (**Fig. 1d–f**), suggesting an anxiogenic-like effect. Notably, the anxiogenic-like effect disappeared in nNOS-knockout mice (**Fig. 1g,h**). Moreover, it did not change

[1]Laboratory of Cerebrovascular Disease, Key Laboratory of Cardiovascular Disease and Molecular Intervention, Nanjing Medical University, Nanjing, China. [2]Department of Pharmacology, Nanjing Medical University, Nanjing, China. [3]Department of Medicinal Chemistry, Nanjing Medical University, Nanjing, China. [4]Department of Neurobiology, Nanjing Medical University, Nanjing, China. [5]Department of Chemistry, Nanjing Medical University, Nanjing, China. [6]Center of Drug Metabolism & Pharmacokinetics, Jiangsu Simcere Pharmaceutical, Nanjing, China. [7]Present address: Key Laboratory of Developmental Genes and Human Disease, Ministry of Education, Institute of Life Sciences, Southeast University, Nanjing, China. [8]These authors contributed equally to this work. Correspondence should be addressed to D.-Y.Z. (dyzhu@njmu.edu.cn) or C.-X.L. (chunxialuo@njmu.edu.cn).

Received 5 February; accepted 27 June; published online 17 August 2014; doi:10.1038/nm.3644

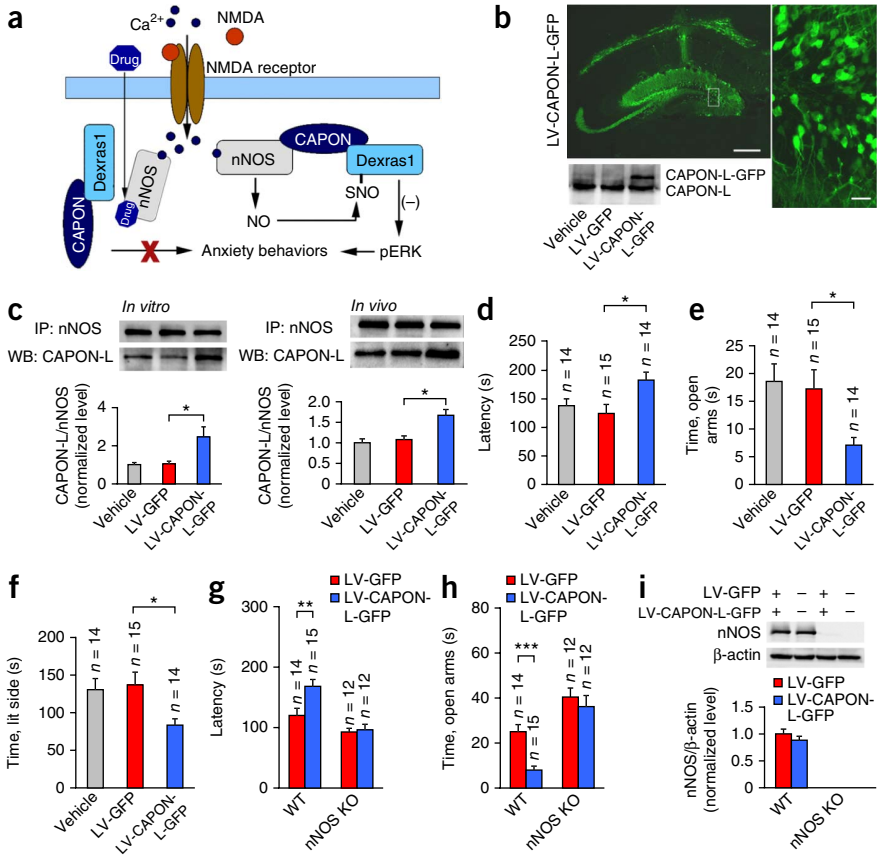

Figure 1 Augmenting nNOS-CAPON interaction causes anxiogenic-like behaviors. (**a**) The hypothesis: nNOS-CAPON interaction modulates anxiety-related behaviors via Dexras1-ERK signaling, and blocking the interaction by drugs has anxiolytic effects. (**b**) Left, a representative of 4 fluorescence images of CAPON-L-GFP expression in LV-CAPON-L-GFP–infected hippocampus of ICR mice. Scale bar, 400 μm. Right, a magnified image from the boxed area in the left image. Scale bar, 30 μm. A representative of 4 immunoblotsare also shown. (**c**) nNOS-CAPON complex levels (presented as the ratio of CAPON-L to nNOS in coimmunoprecipitation) in cultured hippocampal neurons treated by LV-CAPON-L-GFP or LV-GFP for 4 d ($n = 3$, $F_{2,6} = 7.30$, $^*P = 0.047$) or in the hippocampus of mice 10 d after intrahippocampal microinjection of LV-CAPON-L-GFP or LV-GFP ($n = 3$, $F_{2,6} = 11.15$, $^*P = 0.023$). IP, immunoprecipitation; WB, western blot. (**d**–**f**) Latency in the NSF test ($F_{2,40} = 3.99$, $^*P = 0.035$) (**d**), time spent in open arms in the EPM test ($F_{2,40} = 5.21$, $^*P = 0.040$) (**e**) and time spent in lit compartment of the light-dark box ($F_{2,40} = 4.36$, $^*P = 0.033$) (**f**) in ICR mice treated by intrahippocampal microinjection of LV-CAPON-L-GFP, LV-GFP or vehicle (enhanced infection solution). (**g**,**h**) Latency in the NSF test (**g**) and time spent in open arms in the EPM test (**h**) in nNOS-knockout (KO) and WT mice (for NSF test, $F_{1,49} = 8.12$, $^{**}P = 0.0064$; for EPM test, $F_{1,49} = 12.66$, $^{***}P = 0.0008$) treated with LV-CAPON-L-GFP or LV-GFP. (**i**) Immunoblots showing nNOS levels in hippocampus infected with LV-CAPON-L-GFP ($n = 4$, $P > 0.05$). The behaviors in **d**–**h** were assessed 14 d after treatment. In **c**–**i**, analysis of variance (ANOVA) was used for statistical analyses and data are presented as means ± s.e.m.

nNOS levels in the hippocampus in wild-type (WT) mice (**Fig. 1i**). Selectively overexpressing CAPON-L in neurons by intrahippocampal microinjection of AAV-CAPON-L-GFP also produced anxiogenic-like effects in ICR mice (**Supplementary Fig. 3a–f**). Collectively, these data implicate nNOS-CAPON coupling in anxiogenic-like behaviors.

The C-terminal 125 amino acids of CAPON-L specifically interact with nNOS[10]. We thus generated a lentiviral vector, LV-CAPON-125C-GFP, that expresses CAPON-125C and GFP. Intrahippocampal infusion of LV-CAPON-125C-GFP into ICR mice produced considerable CAPON-125C-GFP expression and blocked nNOS-CAPON binding (**Fig. 2a**). It also caused the mice to display significantly decreased latency in the NSF test and increased time spent in open arms in the EPM test, and they crossed the inner fields of the arena significantly more frequently in the open-field (OF) test and spent more time in the lit compartment of the light-dark box (**Fig. 2b,c**). Selectively overexpressing CAPON-125C in neurons by intrahippocampal microinjection of AAV-CAPON-125C-GFP also produced anxiolytic-like effects (**Supplementary Fig. 3a–f**).

The C-terminal 20 amino acids of CAPON-L are essential for its ability to serve as a competitor for nNOS binding to other proteins[10]. We thus generated a lentiviral vector, LV-GFP-CAPON-20C, that expresses CAPON-20C and GFP. Intrahippocampal infusion of LV-GFP-CAPON-20C produced behavioral effects similar to those caused by LV-CAPON-125C-GFP in WT mice but had no effect in nNOS-knockout mice (**Supplementary Fig. 3g–o**).

The C-terminal 12 amino acids of CAPON-L are sufficient for binding to nNOS[21]. Accordingly, we constructed a peptide, Tat-CAPON-12C, comprising CAPON-12C and Tat, a cell-penetrating peptide[22]. Intrahippocampal microinjection of Tat-CAPON-12C selectively blocked nNOS-CAPON binding but not nNOS–PSD-95 binding (**Fig. 2d**). Replacing the penultimate Ala of CAPON-12C with Asp renders it incapable of binding to nNOS[10]. We thus constructed a mutated peptide of 23 amino acids, Tat-CAPON-12C/A22D, as a nonbinding control for Tat-CAPON-12C. Tat-CAPON-12C/A22D did not affect nNOS-CAPON binding and anxiety-related behaviors in ICR mice (**Supplementary Fig. 4a–f**). Tat-CAPON-12C produced anxiolytic-like effects in the NSF, EPM, OF and light-dark box tests in WT mice but had no effects in knockout mice (**Fig. 2e–h**). Moreover, delivering Tat-CAPON-12C into the amygdala also produced anxiolytic-like effects (**Supplementary Fig. 4g–k**). Together, these findings suggest that uncoupling nNOS-CAPON produces anxiolytic-like effects.

Stress plays a role in the etiology of anxiety[23]. We thus treated ICR mice with chronic mild stress (CMS), an unpredictable chronic stress condition leading to anxiety-like behaviors[24]. CMS enhanced nNOS-CAPON association in the hippocampus but not cortex (**Fig. 3a**), probably owing to the fact that CMS selectively upregulated nNOS and CAPON-L expression in the hippocampus (**Supplementary Fig. 5a–e**). Moreover, corticosterone increased nNOS-CAPON association *in vitro* (**Fig. 3b**). Overexpressing CAPON-125C in the hippocampus reversed CMS-induced nNOS-CAPON binding (**Fig. 3c**) and prevented anxiety-like behaviors in the NSF, EPM, OF and light-dark box tests (**Fig. 3d–g**), although there was no change in nNOS or CAPON expression (**Supplementary Fig. 5f,g**), suggesting that uncoupling nNOS and CAPON prevents stress-induced anxiogenic behaviors.

To find small molecules selectively uncoupling nNOS and CAPON, we designed and synthesized a series of compounds (**Fig. 4a**) based

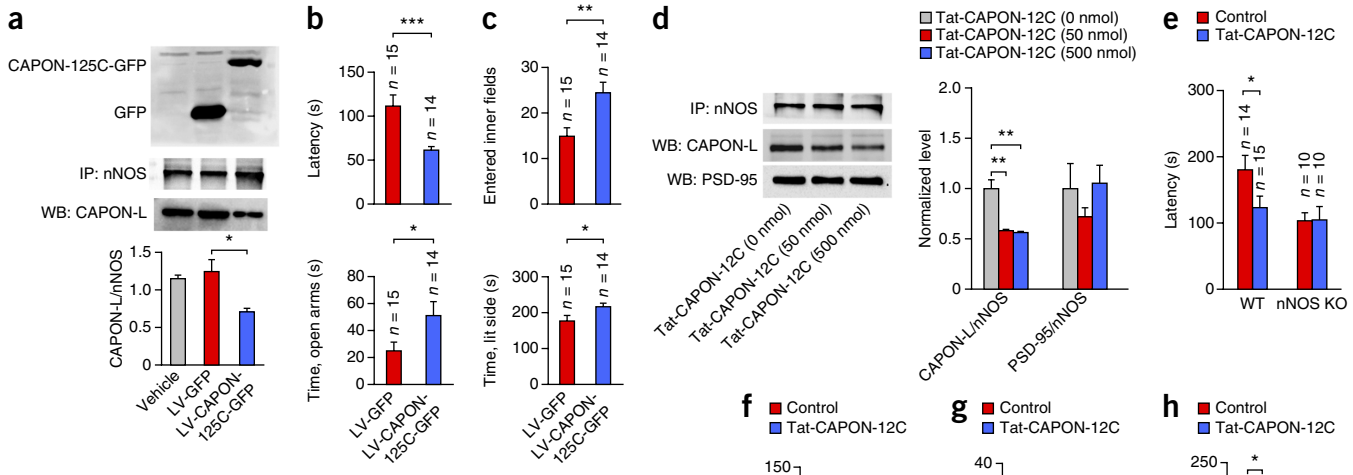

Figure 2 Uncoupling nNOS and CAPON produces anxiolytic-like effects. (**a**) Immunoblots showing CAPON-125C expression (top) and nNOS-CAPON complex levels (presented as the ratio of CAPON-L to nNOS in coimmunoprecipitation) (bottom) in hippocampus from ICR mice infected with LV-CAPON-125C-GFP or LV-GFP ($n = 3$, $F_{2,6} = 8.68$, $^{*}P = 0.023$, ANOVA). (**b**) Latency in the NSF test ($F_{1,27} = 15.97$, $^{***}P < 0.001$) and time spent in open arms in the EPM test ($F_{1,27} = 4.26$, $^{*}P = 0.049$) (two-tailed *t*-test). (**c**) The number of entered inner fields in the OF test ($F_{1,27} = 9.73$, $^{**}P = 0.004$) and time spent in the lit compartment of the light-dark box ($F_{1,27} = 5.40$, $^{*}P = 0.028$) in ICR mice treated by intrahippocampal microinjection with LV-CAPON-125C-GFP or LV-GFP (two-tailed *t*-test). (**d**) Coimmunoprecipitation showing nNOS-CAPON and nNOS–PSD-95 complex levels (presented as the ratio of CAPON-L to nNOS and PSD-95 to nNOS, respectively) in the hippocampus at day 3 after microinjection of Tat-CAPON-12C ($n = 4$, $F_{2,9} = 18.75$, $^{**}P = 0.002$, 0 versus 50 nmol; $^{**}P = 0.001$, 0 versus 500 nmol; ANOVA). (**e**–**h**) Latency in the NSF test (**e**), time spent in open arms in EPM test (**f**), the number of entered inner fields in OF test (**g**) and time spent in lit compartment of the light-dark box (**h**) in KO and WT mice (for **e**, $F_{1,45} = 5.55$, $^{*}P = 0.023$; for **f**, $F_{1,45} = 4.40$, $^{*}P = 0.042$; for **g**, $F_{1,47} = 4.07$, $^{*}P = 0.049$; for **h**, $F_{1,47} = 6.47$, $^{*}P = 0.014$; ANOVA) treated with intrahippocampal microinjection of Tat-CAPON-12C or control (Tat-CAPON-12C/A22D). The behaviors in **b**,**c** and **e**–**h** were assessed 14 d after treatment. Data are presented as means ± s.e.m.

on the chemical mechanism of binding for the C-terminal end of CAPON to the nNOS PDZ domain[21]. Among them, ZLc-002 (*N*-(2-carbomethoxyacetyl)-D-valine methyl ester) was a potent blocker of nNOS-CAPON binding in cultured hippocampal neurons from ICR mice (**Fig. 4b**). *In vivo*, ZLc-002 uncoupled nNOS and CAPON but not nNOS and PSD-95 (**Fig. 4c**).

Next, we infused ZLc-002 into the hippocampus of mice and assessed anxiety-related behaviors 14 d after microinjection. This

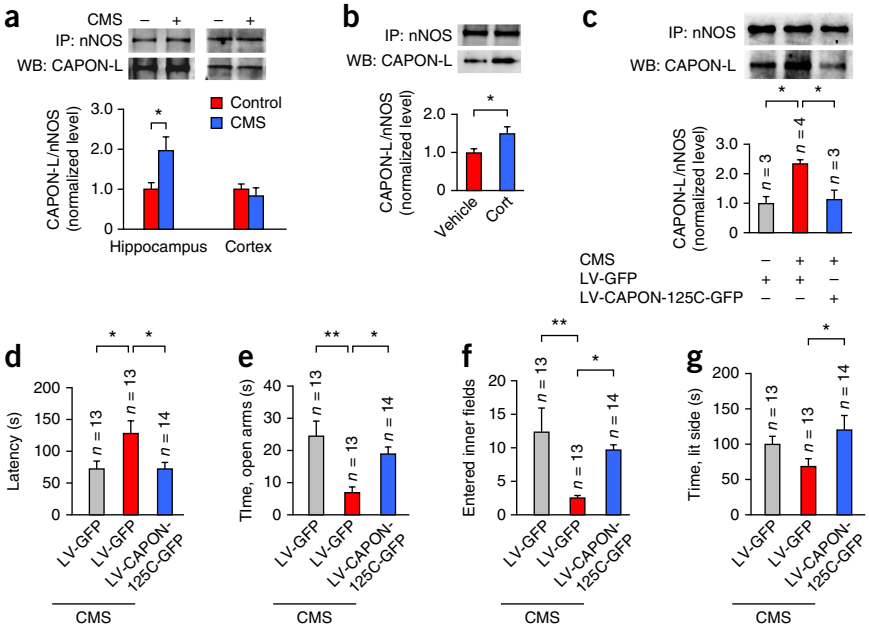

Figure 3 Blocking nNOS-CAPON association reverses stress-induced behavioral modifications. (**a**–**c**) The amounts of nNOS-CAPON complex (presented as the ratio of CAPON-L to nNOS in coimmunoprecipitation) in the hippocampus and cortex of ICR mice exposed to CMS for 21 d (for hippocampus, $n = 4$, $F_{1,6} = 7.02$, $^{*}P = 0.038$; for cortex, $n = 3$, $F_{1,4} = 0.54$, $P = 0.502$, two-tailed *t*-test) (**a**), in cultured hippocampal neurons treated with 10 μM corticosterone (Cort) for 72 h ($n = 4$, $F_{1,6} = 6.40$, $^{*}P = 0.045$, two-tailed *t*-test) (**b**) and in the hippocampus of mice infected with LV-CAPON-125C-GFP and exposed to CMS for 21 d ($F_{2,7} = 11.76$, $^{*}P = 0.011$, LV-GFP/CMS (GC) versus LV-GFP (G); $^{*}P = 0.019$, LV-CAPON-125C-GFP/CMS (CC) versus GC; ANOVA) (**c**). (**d**–**g**) Latency in the NSF test (**d**), time spent in open arms in the EPM test (**e**), the number of entered inner fields in the OF test (**f**) and time spent in lit compartment of the light-dark box (**g**) in ICR mice treated by intrahippocampal microinjection of LV-CAPON-125C-GFP and exposed to CMS for 21 d (for **d**, $F_{2,37} = 5.35$, $^{*}P = 0.028$, GC versus G; $^{*}P = 0.024$, CC versus GC; for **e**, $F_{2,37} = 8.34$, $^{**}P = 0.001$, GC versus G; $^{*}P = 0.033$, CC versus GC; for **f**, $F_{2,37} = 6.47$, $^{**}P = 0.005$, GC versus G; $^{*}P = 0.047$, CC versus GC; for **g**, $F_{2,37} = 3.31$, $^{*}P = 0.049$, CC versus GC; ANOVA). In **c**–**g**, LV-CAPON-125C-GFP was microinjected into the hippocampus at 4 d before starting CMS. Data are presented as means ± s.e.m.

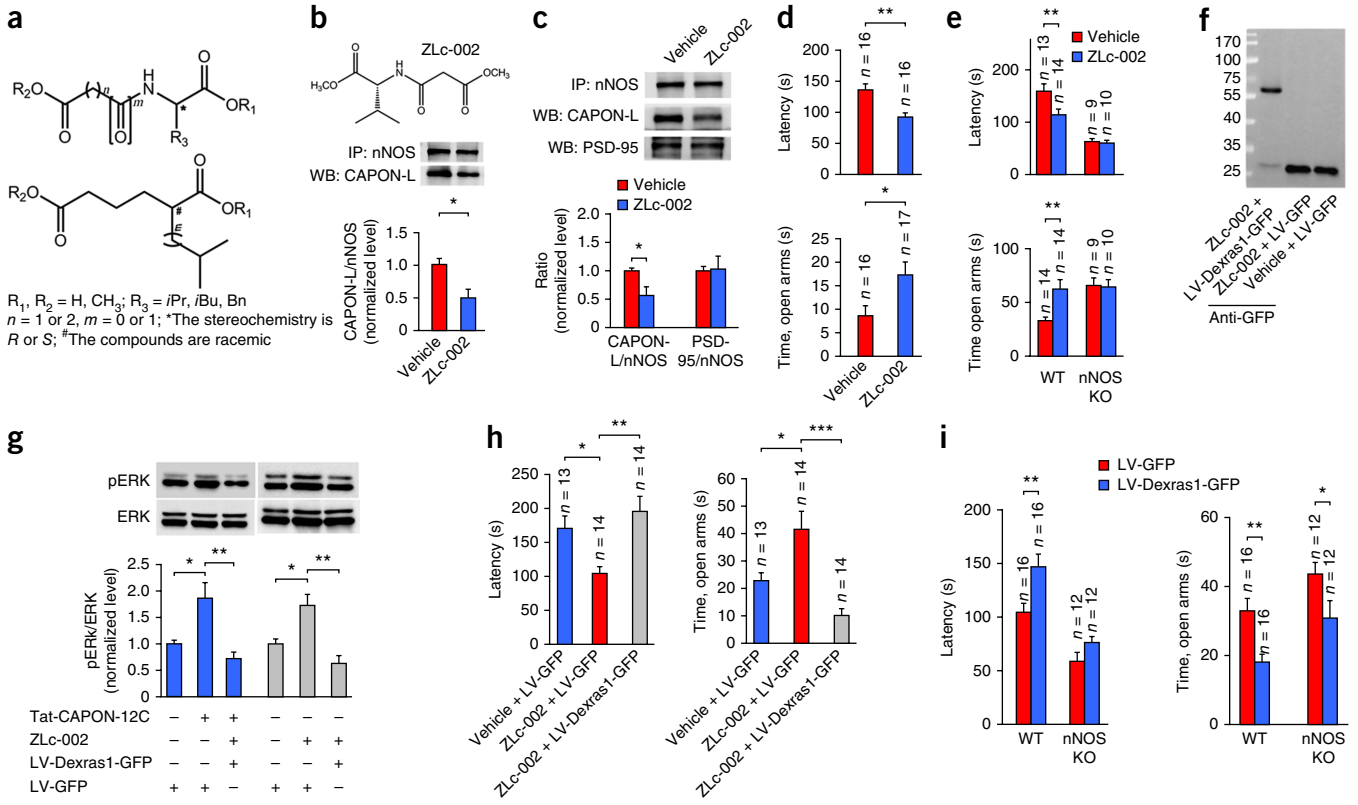

R_1, R_2 = H, CH_3; R_3 = *i*Pr, *i*Bu, Bn
n = 1 or 2, m = 0 or 1; *The stereochemistry is *R* or *S*; #The compounds are racemic

Figure 4 nNOS-CAPON blockers produce anxiolytic-like effects via Dexras1-ERK signaling. (**a**) Structure of target compounds. *i*PR, isopropyl; *i*Bu, isobutyl; Bn, benzyl group. (**b**) nNOS-CAPON complex levels (presented as the ratio of CAPON-L to nNOS in coimmunoprecipitation) in 1.0 μM ZLc-002–treated neurons ($F_{1,4}$ = 9.08, $^*P$ = 0.039, n = 3). (**c**) Coimmunoprecipitation showing nNOS-CAPON ($F_{1,6}$ = 7.43, $^*P$ = 0.034) and nNOS–PSD-95 complex levels (presented as the ratio of CAPON-L to nNOS and PSD-95 to nNOS, respectively) (P > 0.05) in ZLc-002–treated hippocampus from ICR mice (n = 4). (**d**) Latency in NSF test ($F_{1,30}$ = 11.70, $^{**}P$ = 0.002) and time spent in open arms in EPM test ($F_{1,31}$ = 5.79, $^*P$ = 0.022) in ZLc-002–treated ICR mice. In **b**–**d**, two-tailed *t*-test. (**e**) Latency in NSF test ($F_{1,42}$ = 9.64, $^{**}P$ = 0.0034) and time spent in open arms in EPM test ($F_{1,43}$ = 11.41, $^{**}P$ = 0.0016) in ZLc-002–treated WT or KO mice. (**f**–**h**) Dexras1-GFP expression (**f**), pERK and ERK levels in the hippocampus (for Tat-CAPON-12C, $F_{2,12}$ = 10.20, $^*P$ = 0.021, $^{**}P$ = 0.004; for ZLc-002, $F_{2,12}$ = 13.59, $^*P$ = 0.014, $^{**}P$ = 0.001) (n = 5) (**g**) and latency in NSF test ($F_{2,38}$ = 7.17, $^*P$ = 0.040, $^{**}P$ = 0.003) and time spent in open arms in EPM test ($F_{2,38}$ = 12.66, $^*P$ = 0.019, $^{***}P$ < 0.001) (**h**) in LV-Dexras1-GFP–infected ICR mice treated with Tat-CAPON-12C or ZLc-002 (i.v.) for 3 d. (**i**) Latency in NSF test (for WT, $F_{1,52}$ = 10.89, $^{**}P$ = 0.0017; for KO, $F_{1,52}$ = 1.47, P = 0.2314) and time spent in open arms in EPM test (for WT, $F_{1,52}$ = 10.83, $^{**}P$ = 0.0018; for KO, $F_{1,52}$ = 5.73, $^*P$ = 0.0203) in LV-Dexras1-GFP– or LV-GFP–infected mice. In **e**–**i**, ANOVA. Data are presented as means ± s.e.m.

treatment produced significant anxiolytic-like effects in WT mice, as indicated by decreased latency in the NSF test and increased time spent in open arms in the EPM test (**Fig. 4d**), and these anxiolytic-like effects were not present in nNOS-knockout mice (**Fig. 4e**). When we intravenously (i.v.) administered ZLc-002 to ICR mice, it produced anxiolytic-like effects in a dose-dependent manner (**Supplementary Fig. 6a**). Moreover, mice treated with ZLc-002 (i.v.) at a dose of 20 mg kg^{-1} d^{-1} for 3 d displayed anxiolytic-like behaviors (**Supplementary Fig. 6b**), suggesting a rapid onset of action.

Finally, we measured concentrations of ZLc-002 and its theoretical metabolites in serum and brain tissue and found that ZLc-002 was a prodrug, and its hydrolysate ZLc-002-1 (*N*-2-carboxylacetyl-D-valine methyl ester) was the actual performer in the brain (**Supplementary Fig. 6c**–**e**). ZLc-002-1 blocked nNOS-CAPON binding and produced anxiolytic-like effects (**Supplementary Fig. 6f**–**j**). The interaction strength of ZLc-002-1 with the nNOS PDZ domain was substantially larger than with the PSD-95 PDZ domain (**Supplementary Fig. 7**, **Supplementary Tables 1** and **2** and **Supplementary Discussion**), which may explain why ZLc-002 uncoupled nNOS and CAPON but not nNOS and PSD-95. Moreover, there was a correlation between the potencies of ZLc-002 and its analogs in blocking nNOS-CAPON binding and their behavioral effects (**Supplementary Fig. 8**).

To determine how nNOS-CAPON blockers regulate anxiety-related behaviors, we examined phosphorylation of ERK, a kinase that mediates emotional behaviors[17,18,25], and the effects of Dexras1 on pERK. Both Tat-CAPON-12C (3 μmol kg^{-1}) and ZLc-002 (20 mg kg^{-1}) significantly increased pERK abundance in the hippocampus of ICR mice, and overexpressing Dexras1 in the hippocampus reversed their effects on pERK (**Fig. 4f**,**g**) and abolished the behavioral effects of ZLc-002 (**Fig. 4h**). Moreover, overexpressing Dexras1 in the hippocampus partially rescued the anxiolysis found in nNOS-knockout mice (**Fig. 4i**). Lower NO levels in nNOS-knockout hippocampus[26] may explain the weaker behavioral effect of overexpressing Dexras1 in nNOS-knockout compared to WT mice, as Dexras1 activation is physiologically determined by NO[8]. Thus, Dexras1-ERK signaling is crucial for the role of nNOS-CAPON association.

Anxiety is associated with neuroanatomic changes in the hippocampus[27–29]. Treatment of ICR mice with ZLc-002 increased dendritic spine density and function and length and branching of dendrites, and AAV-CAPON-125C-GFP rescued CMS-induced spine loss (**Supplementary Fig. 9a**–**j**). Moreover, nNOS-CAPON blockers increased expression of synapsin and spinophilin, two proteins critical for synaptogenesis[30,31], and the densities of synapsin and PSD-95 double-positive puncta (**Supplementary Fig. 9k**–**o**), implicating nNOS-CAPON in the regulation of synaptogenesis.

nNOS-CAPON blockers are unlikely to work via acute regulation of GABA function because neither Tat-CAPON-12C nor ZLc-002 in the acute hippocampal slices of rats affected GABA inhibitory post-synaptic currents (IPSCs), which are an electrophysiological property of BZDs[32], nor did they have sedative, myorelaxant or incoordination effects, which are frequent behavioral effects of BZDs (**Supplementary Fig. 10a–g**). Moreover, nNOS-CAPON blockers did not affect resting membrane potential of neurons (**Supplementary Fig. 10h–j**). PSD-95 contributes to the modulation of anxiety-related behaviors[33]. However, nNOS-CAPON blockers did not change PSD-95 expression or its association with NMDAR (**Supplementary Fig. 10k–p**). CAPON also binds to synapsins[34] and Dexras1 (ref. 8). ZLc-002 did not affect the interaction of CAPON with synapsins or Dexras1 (**Supplementary Fig. 10q**). Owing to their rapid onset, nNOS-CAPON blockers are pharmacologically different from SSRIs or 5-HT_{1A} receptor agonists, which had no effect until 3–4 weeks after treatment in mice[7]. Moreover, our findings could have wider implications beyond anxiety disorders, as association of nNOS with CAPON in the heart accelerates cardiac repolarization by inhibition of L-type calcium channels[35].

In all of our behavioral experiments, augmenting or disrupting nNOS-CAPON interaction had no effect on appetite, general activity/exploration or locomotor activity (**Supplementary Tables 3–5**, **Supplementary Figs. 1–4**,**6**,**8** and **10**), three possible confounding factors.

In sum, our data highlight the importance of nNOS-CAPON coupling in mediating anxiety-related behaviors and provide a new target for developing potential anxiolytics.

METHODS

Methods and any associated references are available in the online version of the paper.

Note: Any Supplementary Information and Source Data files are available in the online version of the paper.

ACKNOWLEDGMENTS

This work was supported by grants from the National Natural Science Foundation of China (91232304, 81222016, 81030023 and 21303086), the National Basic Research Program of China (973 Program) (2011CB504404) and the Natural Science Foundation of Jiangsu Province–Special Program grant BK2011029 and Distinguished Young Scientist Fund BK20130040, and by the Collaborative Innovation Center For Cardiovascular Disease Translational Medicine. We thank X.D. Qian, H.Y. Ni, F.Y. Zhang, Y. Hu, Y. Tang and Z. Zhu for technical assistance.

AUTHOR CONTRIBUTIONS

L.-J.Z. and C.C. performed the cell culture studies, coimmunoprecipitation, western blotting, surgical preparation and animal behavioral examinations. T.-Y.L. and L.C. contributed the design and synthesis of small-molecule compounds. Y.Z. and H.-H.Z. contributed recombinant lentivirus production and Tat-CAPON-12C preparation. N.J. performed molecular dynamics simulations, interaction energy calculations and force field parameterization for ZLc-002. C.-X.L. contributed to the design of the study. W.L. performed electrophysiological experiments. L.-Y.G., Y.-H.L., Y.M., Q.-G.Z., J.Z. and H.-Y.W. participated in the study. Q.H. and X.-L.H. analyzed concentrations of ZLc-002 and its metabolites. D.-Y.Z. initiated the project, designed the study and wrote the paper. All authors contributed to data analysis.

COMPETING FINANCIAL INTERESTS

The authors declare no competing financial interests.

1. Kessler, R.C. *et al.* Lifetime prevalence and age-of-onset distributions of DSM-IV disorders in the National Comorbidity Survey Replication. *Arch. Gen. Psychiatry* **62**, 593–602 (2005).
2. Tye, K.M. *et al.* Amygdala circuitry mediating reversible and bidirectional control of anxiety. *Nature* **471**, 358–362 (2011).
3. Rupprecht, R. *et al.* Translocator protein (18 kD) as target for anxiolytics without benzodiazepine-like side effects. *Science* **325**, 490–493 (2009).
4. Zhou, Q.G. *et al.* Hippocampal neuronal nitric oxide synthase mediates the stress-related depressive behaviors of glucocorticoids by downregulating glucocorticoid receptor. *J. Neurosci.* **31**, 7579–7590 (2011).
5. Reif, A. *et al.* A neuronal nitric oxide synthase (NOS-I) haplotype associated with schizophrenia modifies prefrontal cortex function. *Mol. Psychiatry* **11**, 286–300 (2006).
6. Nelson, R.J. *et al.* Behavioural abnormalities in male mice lacking neuronal nitric oxide synthase. *Nature* **378**, 383–386 (1995).
7. Zhang, J. *et al.* Neuronal nitric oxide synthase alteration accounts for the role of 5-HT_{1A}-receptor in modulating anxiety-related behaviors. *J. Neurosci.* **30**, 2433–2441 (2010).
8. Fang, M. *et al.* Dexras1: a G protein specifically coupled to neuronal nitric oxide synthase via CAPON. *Neuron* **28**, 183–193 (2000).
9. Zhou, L. *et al.* Treatment of cerebral ischemia by disrupting ischemia-induced interaction of nNOS with PSD-95. *Nat. Med.* **16**, 1439–1443 (2010).
10. Jaffrey, S.R., Snowman, A.M., Eliasson, M.J., Cohen, N.A. & Snyder, S.H. CAPON: a protein associated with neuronal nitric oxide synthase that regulates its interactions with PSD95. *Neuron* **20**, 115–124 (1998).
11. Carrel, D. *et al.* NOS1AP regulates dendrite patterning of hippocampal neurons through a carboxypeptidase E–mediated pathway. *J. Neurosci.* **29**, 8248–8258 (2009).
12. Richier, L. *et al.* NOS1AP associates with Scribble and regulates dendritic spine development. *J. Neurosci.* **30**, 4796–4805 (2010).
13. Lawford, B.R. *et al.* NOS1AP is associated with increased severity of PTSD and depression in untreated combat veterans. *J. Affect. Disord.* **147**, 87–93 (2013).
14. Cheng, H.Y. *et al.* The molecular gatekeeper Dexras1 sculpts the photic responsiveness of the mammalian circadian clock. *J. Neurosci.* **26**, 12984–12995 (2006).
15. Mogha, A., Guariglia, S.R., Debata, P.R., Wen, G.Y. & Banerjee, P. Serotonin 1A receptor–mediated signaling through ERK and PKCα is essential for normal synaptogenesis in neonatal mouse hippocampus. *Transl. Psychiatry* **2**, e66 (2012).
16. Giachello, C.N. *et al.* MAPK/Erk-dependent phosphorylation of synapsin mediates formation of functional synapses and short-term homosynaptic plasticity. *J. Cell Sci.* **123**, 881–893 (2010).
17. Duman, R.S. & Aghajanian, G.K. Synaptic dysfunction in depression: potential therapeutic targets. *Science* **338**, 68–72 (2012).
18. Duric, V. *et al.* A negative regulator of MAP kinase causes depressive behavior. *Nat. Med.* **16**, 1328–1332 (2010).
19. Xu, B. *et al.* Increased expression in dorsolateral prefrontal cortex of CAPON in schizophrenia and bipolar disorder. *PLoS Med.* **2**, e263 (2005).
20. Brzustowicz, L.M. NOS1AP in schizophrenia. *Curr. Psychiatry Rep.* **10**, 158–163 (2008).
21. Tochio, H., Zhang, Q., Mandal, P., Li, M. & Zhang, M. Solution structure of the extended neuronal nitric oxide synthase PDZ domain complexed with an associated peptide. *Nat. Struct. Biol.* **6**, 417–421 (1999).
22. Schwarze, S.R., Ho, A., Vocero-Akbani, A. & Dowdy, S.F. *In vivo* protein transduction: delivery of a biologically active protein into the mouse. *Science* **285**, 1569–1572 (1999).
23. Martinowich, K., Manji, H. & Lu, B. New insights into BDNF function in depression and anxiety. *Nat. Neurosci.* **10**, 1089–1093 (2007).
24. Parihar, V.K., Hattiangady, B., Kuruba, R., Shuai, B. & Shetty, A.K. Predictable chronic mild stress improves mood, hippocampal neurogenesis and memory. *Mol. Psychiatry* **16**, 171–183 (2011).
25. Pucilowska, J., Puzerey, P.A., Karlo, J.C., Galán, R.F. & Landreth, G.E. Disrupted ERK signaling during cortical development leads to abnormal progenitor proliferation, neuronal and network excitability and behavior, modeling human neuron-cardio-facial-cutaneous and related syndromes. *J. Neurosci.* **32**, 8663–8677 (2012).
26. Hu, Y. *et al.* Hippocampal nitric oxide contributes to sex difference in affective behaviors. *Proc. Natl. Acad. Sci. USA* **109**, 14224–14229 (2012).
27. Soetanto, A. *et al.* Association of anxiety and depression with microtubule-associated protein 2- and synaptopodin-immunolabeleddendrite and spine densities in hippocampal CA3 of older humans. *Arch. Gen. Psychiatry* **67**, 448–457 (2010).
28. Mucha, M. *et al.* Lipocalin-2 controls neuronal excitability and anxiety by regulating dendritic spine formation and maturation. *Proc. Natl. Acad. Sci. USA* **108**, 18436–18441 (2011).
29. Lonetti, G. *et al.* Early environmental enrichment moderates the behavioral and synaptic phenotype of MeCP2 null mice. *Biol. Psychiatry* **67**, 657–665 (2010).
30. Kao, H.T. *et al.* A third member of the synapsin gene family. *Proc. Natl. Acad. Sci. USA* **95**, 4667–4672 (1998).
31. Ryan, X.P. *et al.* The Rho-specific GEF Lfc interacts with neurabin and spinophilin to regulate dendritic spine morphology. *Neuron* **47**, 85–100 (2005).
32. Xu, J.Y. & Sastry, B.R. Benzodiazepine involvement in LTP of the GABA-ergic IPSC in rat hippocampal CA1 neurons. *Brain Res.* **1062**, 134–143 (2005).
33. Feyder, M. *et al.* Association of mouse *Dlg4* (PSD-95) gene deletion and human *DLG4* gene variation with phenotypes relevant to autism spectrum disorders and Williams' syndrome. *Am. J. Psychiatry* **167**, 1508–1517 (2010).
34. Jaffrey, S.R., Benfenati, F., Snowman, A.M., Czernik, A.J. & Snyder, S.H. Neuronal nitric-oxide synthase localization mediated by a ternary complex with synapsin and CAPON. *Proc. Natl. Acad. Sci. USA* **99**, 3199–3204 (2002).
35. Chang, K.C. *et al.* CAPON modulates cardiac repolarization via neuronal nitric oxide synthase signaling in the heart. *Proc. Natl. Acad. Sci. USA* **105**, 4477–4482 (2008).

ONLINE METHODS

Animals. Young adult (6- to 7-week-old) male homozygous nNOS-deficient mice (B6;129S4-*Nos1*^{tm1Plh}, knockout, stock number: 002633) and their wild-type controls of similar genetic background (B6129SF2, WT) (both from Jackson Laboratories; maintained at Model Animal Research Center of Nanjing University, Nanjing, China), young adult (6–7 weeks) and newborn (postnatal day P0–P1) ICR mice, and Sprague Dawley (2- to 3-week-old) rats (from Shanghai Slac Laboratory Animal Co. Ltd, Shanghai, China) were used in this study. The mice were maintained at a controlled temperature (20 ± 2 °C) and group housed (12-h light/dark cycle) with access to food and water *ad libitum*. All procedures involving the use of animals were approved by the Institutional Animal Care and Use Committee of Nanjing Medical University. Every effort was made to minimize the number of animals used and their suffering.

Drugs and their injections. Stereotaxic surgery was used to deliver 50 nM Tat-CAPON-12C, 10 μM ZLc-002, 10 mM DETA/NONOate, 0.25 or 2.5 μM Tat-NR2B9C into the dentate gyrus (DG) of the hippocampus at coordinates: 2.3 mm posterior to bregma, 1.3 mm lateral to the midline and 2.0 mm below dura[36] (an intermediate region that has partly overlapping characteristics with dorsal and ventral[37]), and 50 nM Tat-CAPON-12C into the amygdala at coordinates: 1.5 mm posterior to bregma, 3.5 mm lateral to the midline and 4.0 mm below dura. Mice were anesthetized with 0.07 ml of a mixture of ketamine (90.9 mg ml^{-1}) and xylazine (9.1 mg ml^{-1}). Drug solution (2 μl) was microinjected (0.2 μl min^{-1}).

Chronic mild stress procedure and behavioral tests. The procedure of chronic mild stress (CMS) was designed, and NSF, OF and EPM tests were performed as described by our previous studies[4,7]. The light/dark exploration test was performed by placing a mouse in a cage that has two chambers: one lit and one dark compartment. Transitions between sides and the time spent in each division were recorded for 5 min. Myorelaxant in the horizontal wire test and motor incoordination in the rotarod test have been used to assess behavioral effects of BZDs[38]. For horizontal wire test, animals were trained in two separate sessions the day before. On the day of the assay, animals were injected with vehicle or drug and the number of animals unable to grasp the wire was recorded as a measure of myorelaxation[39]. The rotarod test used an apparatus consisting of an elevated cylinder (3.0 cm diameter). Before drug administration, mice were trained to stay on the rotarod revolving at 16 r.p.m. for two consecutive 120-s trials. Drugs were intravenously administered 30 min before test. The duration of time the mice remained on the rotarod was recorded. The maximum duration of a trial was 120 s (ref. 40). Investigators were blinded to group allocation when assessing animal behaviors.

Culture of hippocampal neurons, western blot and coimmunoprecipitation. The culture of hippocampal neurons, the coimmunoprecipitation for protein-protein complexes and western blot analysis of samples from cultured hippocampal neurons and tissues of animals were performed as described by our previous studies[7,9].

Immunocytochemistry and synaptic puncta. Neurons at 7 DIV were treated with 10 μM ZLc-002 or vehicle for 3 d. At 10 DIV, neurons were fixed and incubated with primary antibodies overnight at 4 °C, followed by incubation with the secondary antibodies Cy3 (goat anti-rabbit, Jackson ImmunoResearch, 1:200, 111-165-003) and dylight 488 (goat anti-mouse, Jackson ImmunoResearch, 1:400, 115-483-003)) for 1 h. Images were captured with a confocal laser-scanning microscope (LSM700, Zeiss) and analyzed with Imaris 7.3.0 software (Bitplane Scientific Software, Zurich, Switzerland). Immunopositive puncta along dendrites and synapsin/PSD-95 double-positive puncta were counted. For immunocytochemistry, antibodies to synapsin I (rabbit polyclonal, 1:300; Abcam, ab64581) and PSD-95 (mouse monoclonal, Abcam, 1:300, ab2723) were used. Only PSD-95 puncta with directly adjacent synapsin puncta were scored as colocalized synapsin/PSD-95 puncta.

Golgi-Cox staining. The fresh brains without perfusion were used for Golgi-Cox staining with FD Rapid GolgiStain Kit (FD NeuroTechnologies, Columbia, MD, USA) according to the user manual. Briefly, the brains were first placed in impregnation solution for 2 weeks followed by 2 d in 30% sucrose. Then they were cut into 100-μm coronal sections using a vibratome (World Precision Instruments, Sarasota, FL, USA) and stained. The total number of dendritic branches was counted at each order away from the cell body or dendritic shaft. To calculate spine density of Golgi-stained neurons in the DG, a length of dendrite was traced, the exact length of the dendritic segment was calculated and the number of spines along that length was counted. Ten neurons randomly for each sample were measured, and the average was regarded as the final value of one sample.

Sholl analysis. Images of Golgi-stained neurons were captured with a Zeiss Axio microscope using a 40× objective. Each neuron was reconstructed using Imaris 7.5.2 software, and all analyses were performed using the ImageJ Sholl Analysis Plugin; the center of all concentric circles was defined as the center of cell soma. The starting radius was 15 μm for neurons *in vivo* and 20 μm for neurons *in vitro*, and the ending radius was 150 μm for neurons *in vivo* and 200 μm for neurons *in vitro* from the center; the interval between consecutive radii was 15 μm or neurons *in vivo* and 20 μm for neurons *in vitro*.

Recombinant lentiviruses, neuron specific adeno-associated viruses and their stereotaxic injections. The coding sequences of mouse CAPON-20C, CAPON-125C, CAPON-L and Dexras1 were amplified by RT-PCR. The primers were as follows. For CAPON-20C, forward: 5′-CGGGTACCGGTCGCCACCATGGTGAGCAAGGGCGAGGAG-3′, reverse: 5′-CGGAATTCTCACACGGCGATCTCATCATCCAAACTGTCACCCAACTCCTGCCGCTGTAG-3′; for CAPON-125C, forward: 5′-GAGGATCCCCGGGTACCGGTCGCCACCATGATCACCTTCCGTTCAGG-3′, reverse: 5′-TCACCATGGTGGCGACCGGCACGGCGATCTCATCATCC-3′; for CAPON-L, forward: 5′-GAGGATCCCCGGGTACCGGTCGCCACCATGCCCAGCAAAACCAAGTACAACCTTGTGG-3′, reverse: 5′-TCACCATGGTGGCGACCGGCACGGCGATCTCATCATC-3; for Dexras1, forward: 5′-GAGGATCCCCGGGTACCGGTCGCCACCATGAAACTGGCCGCGATG-3′, reverse: 5′-TCACCATGGTGGCGACCGGACTGATGACACAGCGCTCCT-3′. The PCR fragments and the pGC-FU plasmid were digested with AgeI and then ligated with T4 DNA ligase. GFP was fused to the C-terminus of CAPON-125C, CAPON-L and Dexras1 and fused to the N-terminus of CAPON-20C. Using 100 μl Lipofectamine 2000, 293T cells were co-transfected with 20 μg of the pGC-FU plasmid with a target cDNA, 15 μg of the pHelper1.0 plasmid and 10 μg of the pHelper 2.0 plasmid to generate the recombinant lentiviruses LV-GFP-CAPON-20C, LV–CAPON-125C–GFP, LV-CAPON-L-GFP and LV-Dexras1-GFP.

The shRNA of Dexras1 was constructed and synthesized by Shanghai GeneChem Co., Ltd. (Shanghai, China). The target sequence used against mouse Dexras1 was as follows: 5′-AGGACTAATAATAGGGCAT-3′. Recombinant lentivirus LV-Dexras1-shRNA-GFP was produced by cotransfecting 293T cells with the lentivirus expression plasmid and packaging plasmids using Lipofectamine 2000.

To produce neuron-specific rAAV, CAPON-L and CAPON-125C genes were sub-cloned into pAOV.SYN.EGFP.3FLAG plasmids to produce pAOV.SYN.CAPON-L.EGFP.3FLAG or pAOV.SYN.CAPON-125C.EGFP.3FLAG (Neuron Biotech Co., Ltd, Shanghai, China), which has a neuron-specific promoter, the human synapsin I promoter (hSyn), the 469-bp human sequence chrX:47,364,154-47,364,622. rAAV AAV-CAPON-L-GFP or AAV-CAPON-125-GFP was produced by transfection of AAV-293 cells with pAOV.SYN.CAPON-L.EGFP.3FLAG or pAOV.SYN.CAPON-125C.EGFP.3FLAG, AAV helper plasmid (pAAV Helper) and AAV Rep/Cap expression plasmid. Viral particles were purified by an iodixanol step-gradient ultracentrifugation method. The genomic titer was 2.5–3.5 × 10^{12} genomic copies per ml determined by quantitative PCR.

Intrahippocampal microinjection of recombinant LV or AAV was carried out using a stereotaxic instrument.

Biotin-switch assay. This assay was performed as previously described[7]. Briefly, hippocampi were homogenized in the solution (HEN buffer, 1% NP-40, 0.5 mM PMSF and protease inhibitors, pH 7.4). Free cysteines were blocked in blocking buffer (HEN buffer plus 2.5% SDS, HENS, 200 mM methyl

methanethiosulfonate). Proteins were precipitated with acetone at −20 °C and resuspended in 300 µl HENS solution. After adding 20 mM fresh ascorbic acid and 1 mM biotin-HPDP, proteins were incubated at room temperature for 1 h. After separation using an SDS-PAGE gel in non-reducing loading buffer, biotinylated proteins were detected by immunoblotting. Alternatively, biotinylated proteins were resuspended in 250 µl HENS buffer plus 500 µl neutralization buffer and precipitated with 50 µl prewashed avidin-affinity resin beads at room temperature for 1 h. The beads were washed five times at 4 °C using neutralization buffer containing 600 nM NaCl. Biotinylated proteins were eluted using 30 µl elution buffer and heated at 100 °C for 5 min in reducing SDS-PAGE loading buffer.

Electrophysiological recordings. *GABA IPSCs*. Male Sprague-Dawley (SD) rats, 2–3 weeks old, were anesthetized with ethyl ether and decapitated. The entire hippocampus was removed from the brain. Coronal brain slices (400-µm thickness) were cut using a vibrating blade microtome in ice-cold artificial CSF (ACSF, bubbled continuously with carbogen, pH 7.4). Fresh slices were incubated in a chamber with carbogenated ACSF and recovered at 34 °C for at least 1 h, before they were transferred to a recording chamber. A bipolar electrode (World Precision Instruments) was used to stimulate (100-µs duration) the Schaffer's fibers input to the CA1. The stimulus intensity (~30 µA) was maintained for all experiments. To examine the evoked synaptic transmission, a train of 20 stimuli was delivered at 0.1 Hz. IPSCs were recorded in ACSF perfusion medium containing kynurenic acid (3 mM), which blocks ionotropic glutamate-mediated currents. CA1 neurons were viewed under upright microscopy (Olympus X51W, Nomasky) and recorded with an Axopatch-700B amplifier (Molecular Devices). Drugs were used at following final concentrations: bicuculline (20 µM), ZLc-002 (0, 10 or 100 µM), Tat-CAPON012C (50 or 500 nM), control peptide Tat-CAPON-12Ca-d (500 nM). Data were low-pass filtered at 2 kHz and acquired at 5–10 kHz. The series resistance (R) was always monitored during recording for fear of resealing the ruptured membrane, which will cause changes in both the kinetics and amplitude of the IPSCs. Cells in which the R or capacitance deviated by >20% from initial values, or R > 20 MΩ at any time during the recording, were excluded from the analysis. Data were collected with pClamp 10.3 software and analyzed using Clampfit 10.3 (Molecular Devices).

GABA-evoked currents. CA1 neurons of hippocampal slices from rats were viewed under upright microscopy (Olympus X51W, Nomasky) and recorded with Axopatch-200B amplifier (Axon Instrument). GABAergic responses were evoked by perfusing slices with GABA for 2 min. After GABA washout, the slices were sequentially perfused with drugs to examine their effects on GABA responses. Data were low-pass filtered at 2 KHz and acquired at 5–10 KHz. The series resistance (R) was always monitored during recording for fear that reseal of ruptured membrane would cause change of both kinetics and amplitude. Cells in which Rs or capacitance deviated by >20% from initial values, or Rs > 20 MΩ at any time during the recording, were excluded from analysis.

Resting membrane potentials. We measured resting membrane potential of CA1 neurons using the reversal potential of K^+ currents through cell-attached patches. Microelectrodes (4–6 MΩ) were filled with the following solution (in mM): potassium gluconate 120, KCl 15, $MgCl_2$ 4, EGTA 0.1, HEPES 10.0, MgATP 4, Na_3GTP 0.3, phosphocreatine 7 (pH 7.4, 300 mOsm). The junction potential between pipette and extracellular solution was nulled by the voltage-offset of the amplifier before establishing the seal and was not further corrected. Depolarizing voltage ramps (from V_h = −100 to +100 mV) were applied to activate voltage-gated K^+ channels and to establish the K^+ current reversal potential. Between stimulations, the patch was held at −65 mV hyperpolarized with respect to Vm to remove possible voltage-dependent 'steady-state' inactivation from the K(V) channel at the physiological Vm. For analysis of currents evoked by ramp stimulation, a correction was made for a leak component by linear extrapolation of the closed level below the threshold for activation of the voltage-gated current.

Miniature EPSCs. Whole-cell recordings were made from cultured hippocampal neurons (12–15 DIV, plating density: 1×10^5 cm^2) from rats using low-resistance pipets (4–8 MΩ). The membrane potential was held at −65 mV with the following intercellular solution (in mM): CsF 140; BAPTA 10; $CaCl_2$ 1.0; $MgCl_2$ 2.0; HEPES 10.0; and K_2ATP_4 (pH 7.3). The series resistance was monitored throughout the experiment and if it varied by more than 10%, the experiment were rejected. The cells were continuously perfused with extracellular solution at 28–32 °C that contained (in mM): NaCl 140, $CaCl_2$ 1.3, KCl 5.0, HEPES 25, glucose 33, bicuculline methiodide 0.02, TTX 0.0005 (pH 7.4). mEPSCs were recorded with an Multiclamp 700B amplifier (Axon Instruments, Inc.) and filtered at 2 kHz, and the recording lengths were more than 5 min. Two different preparations were employed. Three cells were recorded from each culture preparation.

Whole-cell recordings from acute hippocampal slices of rats (2 weeks old) were made with patch pipettes containing solutions (in mM): Cs-gluconate 132.5, CsCl 17.5, $MgCl_2$ 2.0, EGTA 0.5, HEPES 10, ATP 4.0 and QX-314 5.0, with the pH adjusted to 7.2 by CsOH. mEPSCs were recorded with TTX (0.0005 mM) and bicuculline methiodide (0.02 mM) perfusing in oxygenated ACSF with an Multiclamp 700B amplifier, and filtered at 2 kHz. The recording lengths were more than 5 min. All data are from 3 animals for control and 4 animals for drug experiments.

Data were analyzed using Mini software (http://www.synaptosoft.com/MiniAnalysis/index.html). Up to 100 events from each cell were selected at a fixed sampling interval to generate cumulative probability plots.

Design and synthesis of ZLc-002. Although CAPON has a C-terminal sequence different from the Asp/Glu-X-Val motif, an optimal nNOS PDZ binding sequence[41], they bind to the same pocket of the nNOS PDZ domain[21]. nNOS PDZ has a conserved 'GLGF' carboxylate-binding motif[42]. Val0 of the C-terminal peptide of CAPON is crucial for binding CAPON to nNOS[10]. The side chain of Val0 of Asp/Glu-X-Val motif points to a hydrophobic pocket formed by the side chains of Leu22, Phe24 and Leu78, and the carboxyl group of Val0 binds strongly to the carboxyl binding motif 'GLGF'. Two additional hydrophobic residues (Ile81 and Val88) located at the perimeter of the pocket also partially interact with the side chain of Val0 in the peptide[21]. Moreover, two basic amino acids, Lys16 and Arg79, are in close proximity to the binding site of valine. If D-valine is placed into the pocket of the nNOS PDZ domain, its carboxyl group will bind to the 'GLGF' motif, its side chain isopropyl will insert to the hydrophobic pocket, and its amino group will turn toward to the direction of Lys16 or Arg79. If we attach a carboxyl group to the amino group of the D-valine through a suitable linker, the additional carboxyl group will form an ionic bond between the carboxylate and positive charge of Lys or Arg. We deduced that the molecule may have a competitive advantage over L-valine for binding to nNOS PDZ because of the ionic bond. We thus designed and synthesized a series of compounds which are derived from condensation of dicarboxylic acids with D- or L-valine methyl ester. The methyl ester compounds may increase lipophilicity and membrane permeability. The amide bond linking the extra-carboxyl group with valine is a relatively rigid linkage. To make the side chain more flexible, and therefore probably more easily orient the carboxyl group to the nearby basic group, we substituted the amide moiety with a carbon chain, and in some compounds the isopropyl was replaced by isobutyl. It was demonstrated by a library screening that the binding pocket for Val of nNOS PDZ can accommodate the larger side chains of Leu and Ile[41]. Thus, molecules with larger side chains of Leu or Phe were also synthesized. Since D-conformation compounds are generally resistant to hydrolysis *in vivo*, there is a possibility that the compounds are hydrolyzed into mono methyl ester compounds but not dicarboxylic acid compounds. In this case, mono methyl ester compounds may also be effective because the oxygen atoms in the ester group can form hydrogen-bonding interactions with the peptide backbone of nNOS PDZ and/or form electrostatic interactions with the side chains of Lys16 or Arg79. The residue numbering in the sequence comes from the Protein Data Bank (PDB id: 1B8Q).

The synthesis of ZLc-002 is outlined as follows. *N*-Methylmorphinline (2 ml) was added dropwise to a solution of D-valine methyl ester hydrochloride (1.50 g) in CH_2Cl_2 (35 ml) under −15 °C. Methyl malonyl chloride (1 ml) was then added and stirred under −15 °C for 30 min, and then at room temperature for 22 h. The solvent was removed under vacuo, and the residue was diluted with 8 ml H_2O. The solution was extracted with EtOAc (50 mL × 4). The combined extracts were washed with 10% citric acid solution, 5% Na_2CO_3 solution and saturated NaCl aqueous solution consecutively. The EtOAc layer was dried over Na_2SO_4,

doi:10.1038/nm.3644

filtered and evaporated to give a yellowish liquid. The product was purified by flash chromatography (SiO_2, EtOAc:PE = 1:2). ^{1}H-NMR (300 MHz,$CDCl_3$) δ (ppm): 0.96 (t, 6H, J = 6.48 Hz), 2.20 (s, 1H), 3.37 (s, 2H), 3.75 (s, 3H), 3.77 (s, 3H), 4.56 (s, 1H), 7.52 (s, 1H).

Other methods. Detailed methodology, including molecular dynamics simulations, interaction energy calculations and force field parameterization for ZLc-002-1, and analysis of drug concentrations in blood and brain, is described in the **Supplementary Methods**.

Statistical analyses. Data are presented as means ± s.e.m. The significance of differences was determined by one-way analysis of variance followed by Scheffe's *post hoc* test. When two factors were assessed, the significance of differences was determined by two-way analysis of variance. χ^2 test was used to compare incidence rate between groups. Differences were considered significant when $P < 0.05$. The sample size was predetermined by analyzing preexperimental data with PASS (power analysis and sample size) software. For animal studies, the sample size was predetermined by our prior experience. Randomization was used in all experiments.

36. Munoz, J.R., Stoutenger, B.R., Robinson, A.P., Spees, J.L. & Prockop, D.J. Human stem progenitor cells from bone marrow promote neurogenesis of endogenous neural stem cells in the hippocampus of mice. *Proc. Natl. Acad. Sci. USA* **102**, 18171–18176 (2005).
37. Fanselow, M.S. & Dong, H.W. Are the dorsal and ventral hippocampus functionally distinct structures? *Neuron* **65**, 7–19 (2010).
38. Rudolph, U. *et al.* Benzodiazepine actions mediated by specific γ-aminobutyric $acid_A$ receptor subtypes. *Nature* **401**, 796–800 (1999).
39. Bonetti, E.P. *et al.* Benzodiazepine antagonist RO 15–1788: neurological and behavioral effects. *Psychopharmacology (Berl.)* **78**, 8–18 (1982).
40. Ren, L. *et al.* $GABA_A$ receptor subtype selectivity underlying anxiolytic effect of 6-hydroxyflavone. *Biochem. Pharmacol.* **79**, 1337–1344 (2010).
41. Stricker, N.L. *et al.* PDZ domain of neuronal nitric oxide synthase recognizes novel C-terminal peptide sequences. *Nat. Biotechnol.* **15**, 336–342 (1997).
42. Doyle, D.A. *et al.* Crystal structures of a complexed and peptide-free membrane protein-binding domain: molecular basis of peptide recognition by PDZ. *Cell* **85**, 1067–1076 (1996).